Journal of Zhejiang University-SCIENCE A (Applied Physics & Engineering)
ISSN 1673-565X (Print); ISSN 1862-1775 (Online)
www.zju.edu.cn/jzus; www.springerlink.com
E-mail: jzus@zju.edu.cn

A destructive field study on the behavior of piles under tension and compression*

Zhong-miao ZHANG[1,2], Qian-qing ZHANG[†‡1,2], Feng YU[3]

([1]*MOE Key Laboratory of Soft Soils and Geoenvironmental Engineering, Zhejiang University, Hangzhou 310058, China*)

([2]*Institute of Geotechnical Engineering, Zhejiang University, Hangzhou 310058, China)*

([3]*School of Civil Engineering and Architecture, Zhejiang Sci-Tech University, Hangzhou 310018, China*)

[†]E-mail: zqq5820948@126.com

Received May 31, 2010; Revision accepted Sept. 20, 2010; Crosschecked Mar. 1, 2011

Abstract: This paper involves a series of destructive full-scale load tests on long bored piles instrumented with strain gauges along the shafts, including two compression and two tension loading tests. The load-displacement response, axial force, skin friction, and the thresholds of the slip displacement for fully mobilizing the skin resistances in different soils are discussed. Moreover, the theoretical solution for estimating the pile tip settlement under compression was adopted to analyze the test results. It was found that the measured skin frictions for the piles under compression were about 6% to 42% higher than the estimated values of the cone penetration tests (CPTs), whereas the measured skin frictions in the uplift cases were about 16% to 50% smaller than the estimated values. In addition, the average limited skin frictions for the tension piles were about 0.36 to 0.78 times the average ultimate skin frictions for the piles under compression. It also can be indicated that the skin friction along the pile depth approached the limited state, and decreased from a peak value with increasing loads.

Key words: Destructive full-scale test, Load-displacement response, Axial force, Pile-soil relative displacement, Skin friction
doi:10.1631/jzus.A1000253 **Document code:** A **CLC number:** TU473.1

1 Introduction

Cast-in-situ bored piles, generally varying from 0.6 to 1.5 m in diameter, have been used worldwide as the foundations of heavy-load structures, because of the relatively low cost and ease of length adjustment during pile installation. The purpose of the piles is to transmit a foundation load to a solid ground, and to resist vertical, lateral, and uplift loads. In the past several decades, many studies have dealt with the analysis of the behaviors of vertically loaded piles, and much effort has been made to develop theoretical methods for the analysis of the behavior of a single pile and a pile group (Randolph and Worth, 1979; Kraft *et al*., 1981; Guo and Randolph, 1999; Xiao *et al*., 2002; Zhu and Chang, 2002; Ai and Han, 2009; Said *et al*., 2009). Meanwhile, prediction of the uplift capacity of a pile is one of the most interesting areas of research in pile foundation designs. Some studies on the behavior of the piles under uplift loads have been conducted (Das 1983; Shanker *et al*., 2007; Lai and Jin, 2010), which were very helpful in predicting the uplift capacity of a pile.

The previous works show that the behaviors of the piles under tension and compression are different because of the differences of the two pile types in load transfer mechanism and skin friction distribution. However, few studies have been concerned with the details of the differences in the behaviors between the tension piles and the compression piles. Furthermore, it should be noted that the above-mentioned studies normally use model pile tests or numerical approaches to analyze the behavior of the piles under

‡ Corresponding author

* Project (No. 51078330) supported by the National Natural Science Foundation of China

tension or compression, and very limited data are available for the destructive field tests of the compression and tension piles. Therefore, there is a need to analyze the behavior of tension piles compared with that of compression piles.

The overall objectives of the full-scale field tests are: (1) to understand the load-displacement response of the pile under tension and compression; (2) to clarify the load transfer mechanism of the pile subjected to vertical and uplift loads; (3) to identify the relationship of or differences between load and skin friction distributions for the pile under tension and compression; and (4) to compare the skin frictions.

2 Site conditions and pile description

The field tests were conducted in Hangzhou, China. The detailed soil profiles and properties are presented in Table 1. The ground water table elevation in this site varied between 0.7 and 1.2 m below the ground surface.

In order to better understand the differences in the tension and compression pile responses, four bored piles with identical diameter and approximate length were tested. Parameters of the piles under tension and compression are summarized in Table 2.

3 Experimental

The setups employed for tension and compression testing of piles are shown in Fig. 1.

A slow maintained-load method was adopted for the tests. The load was applied by the reaction of jacks at the pile top, and was increased step by step. The magnitude of load at each step was selected as 1/8−1/12 of the maximum design load for the test, and the magnitude of the first load step was double that of the subsequent load steps. At each load step, the

Table 1 Soil profiles and properties

Soil No.	Soil layer	w (%)	$E_{s1\text{-}2}$ (MPa)	c (kPa)	φ (°)	f_{su} (kPa)	q_{su} (kPa)	q_{bu} (kPa)
0-1	Plain fill	26.90	10.8	13.7	30.2	100		
0-2	Pond mud	43.30	2.8					
1-1	Clayey silt	28.30	10.8	14.8	28.70	240	28	
1-2	Sandy silt	27.99	11.8	12.6	30.10	280	44	
1-3	Sandy silt	27.10	11.3	11.0	30.30	250	36	
2-1	Sandy silt	26.80	11.8	13.5	29.20	300	46	
2-2	Sandy silt	25.50	10.9	11.1	30.40	260	38	
3-1	Silty sand mixed silt	24.80	11.3	9.6	30.40	320	50	
3-2	Clayey silt	29.38	8.4	15.9	24.30	220	30	
3-3	Silt clay	41.38	3.4	17.2	9.20	170	20	
4-1	Silty clay	27.30	6.5	60.3	15.20	360	54	
4-2	Silty clay	23.65	7.0	54.9	15.77	420	62	
4-3	Silty clay	27.70	5.5			320	54	
5-1	Silty clay mixed sand	22.50	7.1	31.4	22.50	480	68	
5-2	Fine sand	20.58	8.6	15.3	27.74	440	70	
6-1	Gravel					800	80	4000
6-1′	Fine sand	24.90	9.5	4.5	31.50	360	60	
6-2	Gravel					1100	110	5000
6-3	Gravel					1060	120	5400
10-2	Highly-weathered sandstone mixed gravel					900	140	
10-3	Mid-weathered sandstone mixed gravel					2000	200	7000

w is the natural water content; c and φ are the cohesion and internal friction angles of soil, respectively, which are derived from consolidated undrained (CU) triaxial tests; $E_{s1\text{-}2}$ is the compression modulus; f_{su} is the ultimate value of strata bearing capacity; and q_{su} and q_{bu} are the ultimate values of skin friction and tip resistance, respectively, estimated from the cone penetration tests (CPTs)

Table 2 Parameters of piles under tension and compression

Pile No.	Loading type	L (m)	d (m)	T (d)	E_c (GPa)	α_f	Reinforcing bar	
							Diameter (mm)	Number
TS1	Tension	40.2	0.8	68	31.5	1.17	25	30[a], 15[b]
TS2	Tension	40.0	0.8	70	31.5	1.19	25	30[a], 15[b]
TS3	Compression	39.1	0.8	65	33.5	1.19	16	12[a], 6[b]
TS4	Compression	39.2	0.8	66	33.5	1.16	16	12[a], 6[b]

[a] Number of reinforcing bars attached at 20 m above the pile head; [b] Number of reinforcing bars attached at 20 m below the pile head. L: pile length; d: pile diameter; T: time after pile installation; E_c: elastic modulus of concrete; α_f: ratio of actual to theoretical concrete volume

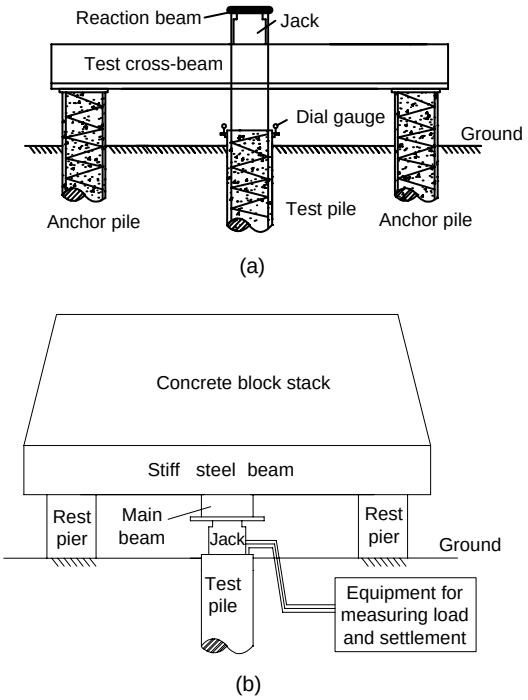

Fig. 1 Tension (a) and compressive load test (b) setups

settlement at the pile head was recorded after the load had been applied and maintained for 5, 15, 30, 45, and 60 min. Thereafter, the settlement was recorded every 30 min. Each load increment was maintained after loading until two consecutive displacements within each hour were less than 0.1 mm. The unloading test was performed by reducing the load in decrements that were twice the loading increments. These requirements were based on the typical criteria recommended by the Chinese Technical Code for Testing of Building Foundation Piles (JGJ 106-2003). For the destructive tests of these four piles, the load tests were not stopped until failure.

To capture the mechanism of load transfer, 24 vibrating wire rebar strain gauges were attached to the steel rebar cage at 8 locations of each pile. Based on the locations of strain gauges, each pile was divided into 8 parts from the pile top to the pile end, as shown in Fig. 2.

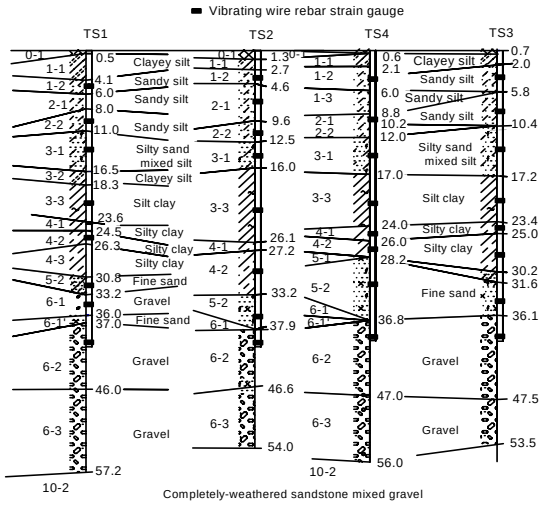

Fig. 2 Distributions of soil and locations of strain gauges (unit: m)

The settlement at the pile head was derived from the dial gauges located at the pile top. The test method for the pile tip settlement is summarized as follows: (1) a 66 mm diameter pipe was attached to the steel reinforcement cage; (2) a 33 mm diameter pipe was placed inside the 66 mm diameter pipe before the loading test was conducted; and (3) the settlement at the pile tip was measured with the dial gauges located on the 33 mm diameter pipe during the loading test.

4 Results and discussion

4.1 Load-displacement responses of piles

The load-displacement curve is a useful tool to establish the ultimate bearing capacity of a single pile under tension or compression. The ultimate bearing capacity of a single pile may be defined as the load when the pile is plunged, or displacement at the pile head increased rapidly under sustained load, as suggested by Prakash and Sharma (1990). Punching failure typically involves settlements that far exceed the acceptable range for design. If the plunging point is not clear, another definition of the ultimate load is needed. The load-displacement responses at the pile head and pile tip of the four piles under tension and compression are shown in Fig. 3.

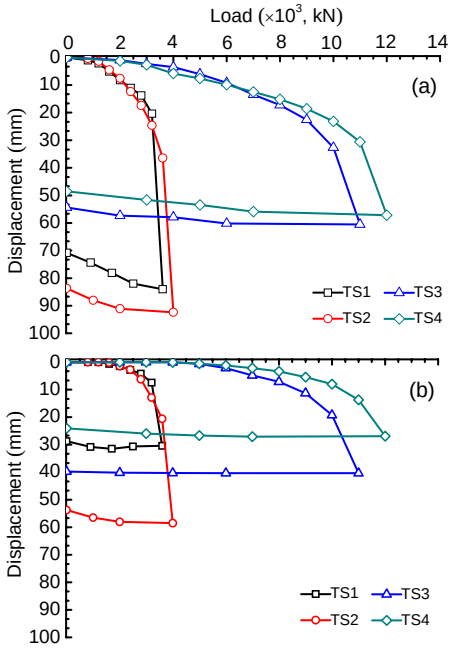

Fig. 3 Load-displacement responses at the pile head (a) and pile tip (b) under tension and compression

Fig. 3 shows that each load-displacement curve has a distinct plunging point, and the ultimate bearing capacity of the pile is taken to be the load that occurs at the onset of the plunging point. The ultimate bearing capacity is also equal to the load prior to reaching the destructive (maximum) load; i.e., when the applied load of the pile TS1 increases from 3200 to 3600 kN, there is a significant increase in displacement at the pile head or pile tip. Punching failure is thereby very likely to occur at the pile tip under a load of 3600 kN. The ultimate bearing capacity of TS1 under tension is assumed to be 3200 kN, and its corresponding displacements at the pile head and tip are 20.4 and 7.4 mm, respectively. Following the above-mentioned criterion, the ultimate bearing capacities of other three piles can be obtained. The proposed ultimate bearing capacity and the displacement at the corresponding capacity for each pile are summarized in Table 3.

Based on the load-displacement responses of the pile, the behavior is found to be different for the piles tested in tension and compression under the destructive load. There are large displacements at the pile head and pile tip in the uplift cases, resulting in pulling up of the whole pile, whereas a punching failure occurs at the pile tip for the piles under compression.

The results in Table 3 show that the ultimate bearing capacities of the piles under tension are about 30% of those under compression. The lower bearing capacity of the pile under tension may result from being without tip resistance and the lower skin frictions being mobilized at the limited displacements.

4.2 Axial forces in piles

Based on the measured vibration frequency of the strain gauge at a certain depth, the calculation method of the average axial force at that depth can be summarized as follows.

Table 3 Ultimate bearing capacities of piles under tension and compression and their corresponding displacements

Pile No.	Loading type	P_{max} (kN)	S_{maxt} (mm)	S_{maxb} (mm)	P_u (kN)	S_{ut} (mm)	S_{ub} (mm)	Failure mode
TS1	Tension	3600	84.0	30.4	3200	20.4	7.4	Pulling up of whole pile
TS2	Tension	4000	92.4	58.5	3600	36.5	20.6	Pulling up of whole pile
TS3	Compression	11 000	60.6	40.3	10 000	32.7	19.2	Punching failure at the pile tip
TS4	Compression	12 000	57.2	26.9	11 000	30.6	13.7	Punching failure at the pile tip

P_{max} is the maximum applied load at the pile head; and S_{maxt} and S_{maxb} are displacements at the pile head and pile tip under the maximum applied load. P_u is the ultimate bearing capacity of the pile; and S_{ut} and S_{ub} are displacements at the pile head and pile tip under P_u

The axial force of the strain gauge located at pile section *i* is evaluated by

$$P_{sgi} = K(F_i^2 - F_0^2) + B, \tag{1}$$

where K is the calibration coefficient of the strain gauge, F_i is the vibration frequency of the strain gauge located at pile section i, F_0 is the initial vibration frequency of the strain gauge before the test is carried out, and B is the zero offset value of the strain gauge.

The strain of the reinforcing steel bar located at pile section *i* can be expressed as

$$\varepsilon_i = P_{sgi} / E_{rb} A_{rb}, \tag{2}$$

where A_{rb} is the reinforcing steel bar area, and E_{rb} is the elastic modulus of the reinforcing steel bar.

Because the steel rebar can be considered fully bonded with concrete, the strain in the steel rebar is assumed to be equal to that in the concrete. The axial force at pile section *i* is expressed by

$$P_i = E_c \cdot \varepsilon_i \cdot A_c, \tag{3}$$

where A_c is the concrete area and E_c is the elastic modulus of the concrete.

The axial force in the piles under tension and compression are shown in Fig. 4.

Fig. 4 shows that the axial force decreases with depth because of skin resistance, but increases with increasing applied loads. For the piles under compression (TS3 and TS4), base load gradually develops with increasing loads at the pile head, whereas the measured tip resistance in uplift cases (TS1 and TS2) is near zero during the whole loading cycle. It should be noted that the dashed curve plotted in Fig. 4 represents the distribution of axial force under the destructive load (3600, 4000, 11 000, and 12 000 kN for the piles TS1, TS2, TS3, and TS4, respectively). Under the destructive load, the applied load at the pile head cannot remain stable, and decreases because of the degradation of skin friction; i.e., the applied loads at the pile head maintain at 3300, 3300, 8000, and 9500 kN for the piles TS1, TS2, TS3, and TS4, respectively.

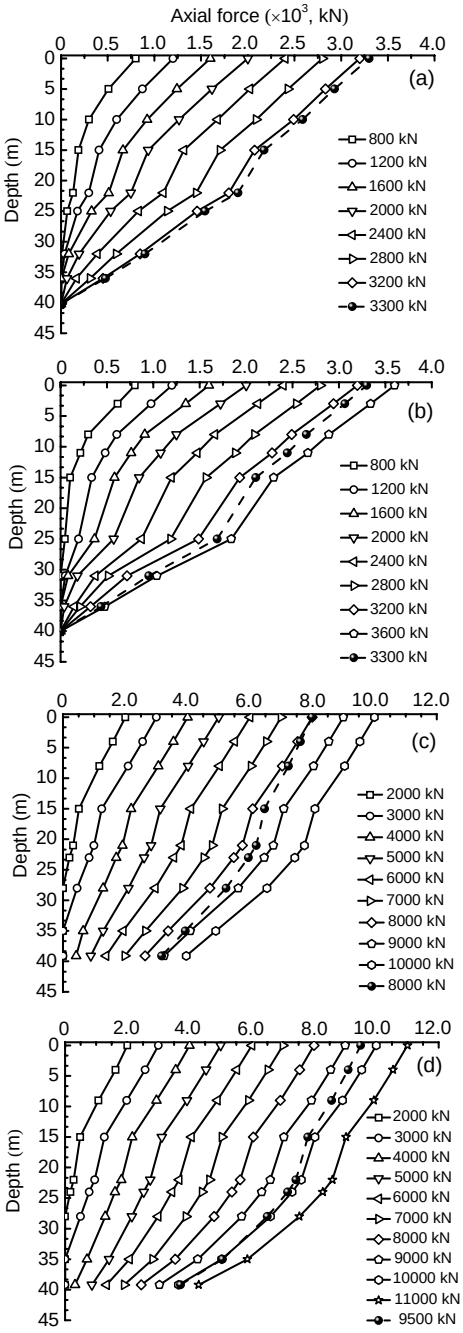

Fig. 4 Axial forces of test piles under different loads
(a) TS1; (b) TS2; (c) TS3; (d) TS4

4.3 Skin friction along piles

Skin friction along each pile under tension or compression can be calculated by dividing the difference of two consecutive axial forces by the pile shaft area between the two strain gauges. Therefore, the skin

friction is an average value corresponding to the distance between the locations of two strain gauges.

As shown in Fig. 5, the skin friction is gradually mobilized from the pile head to the pile tip, and increases with increasing applied loads before the skin friction is fully mobilized. However, when the skin friction is fully developed, the skin friction softening occurs accompanied with a reduction in skin friction. Under the destructive load, the skin frictions decrease to some degree, except for those of the pile TS1 at 25 to 40.2 m depth, due to the relative slip between the pile and soils, as shown of the dashed lines in Fig. 5. This is the main cause of the decrease in the applied loads.

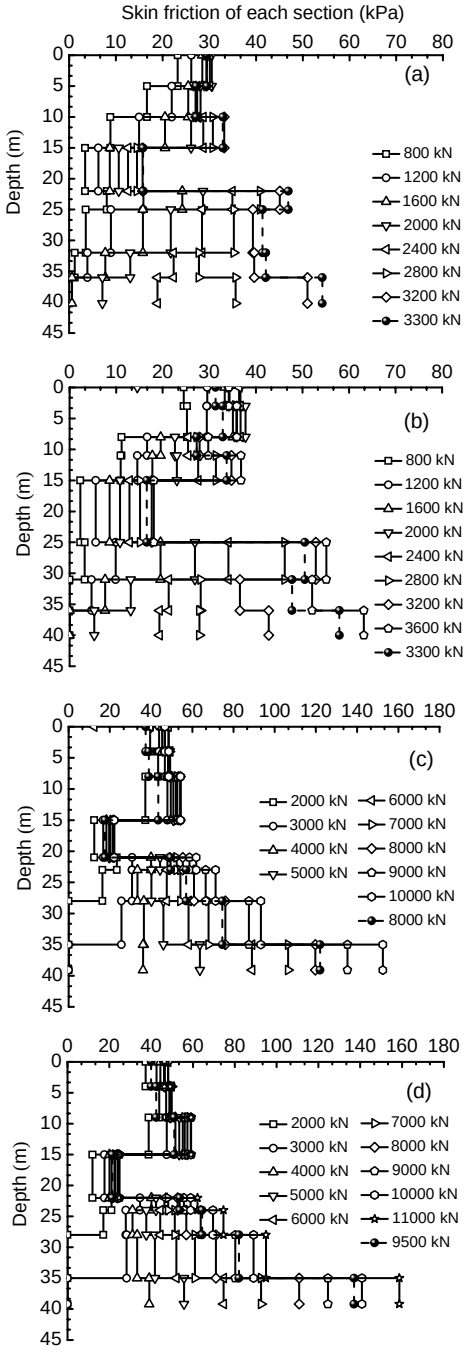

Fig. 5 Distribution of skin friction along piles under different loads

(a) TS1; (b) TS2; (c) TS3; (d) TS4

The measured average skin friction of each soil layer under the ultimate bearing capacity is compared in Table 4 with the values estimated from the cone penetration tests (CPTs) and the values suggested by the Chinese Technical Code for Building Pile Foundations (JGJ 94-2008).

The comparisons show that the measured skin frictions for the piles under compression are about 6% to 42% higher than the values estimated from the CPTs, whereas the measured values of the uplift cases are about 16% to 50% smaller than the estimated values. In addition, the average limited skin frictions for the tension piles are about 0.36 to 0.78 times the average ultimate skin frictions of the piles under compression. It is noted that the average skin frictions of the compression piles are much larger than those of the piles under tension, resulting in higher capacities of the compression piles. That is, the skin frictions in the uplift cases have more limited effects than those in the compression piles, especially for the shaft frictions near the pile tip.

Average skin friction for each pile is determined as being the difference between the load on the pile head and the load on the pile tip divided by the total surface area. The variation in average skin friction with displacement at the pile tip for the four piles is shown in Fig. 6.

Fig. 6 indicates that the tip displacement-average skin friction curve has a distinct turning point at the onset of the destructive load. This is different from the relationship between the tip displacement and the average skin friction in the non-destructive test (Zhang *et al*., 2009; 2010). The average skin friction is gradually mobilized with the development of the tip displacement before the destructive load. The average skin friction under compression is about 1.3 times higher than that under tension. It is likely that larger displacement at the pile tip is required to fully mobilize the skin friction for the piles under compression.

Table 4 Skin friction of each soil layer under the capacity load of piles

Pile No.	q_{su1} (kPa)	q_{su2} (kPa)	q_{su3} (kPa)				R_1		R_2
			TS1	TS2	TS3	TS4	TS1 and TS2	TS3 and TS4	
1-2	24–42	44	29.4	34.2	46.7	46.3	0.723	1.057	0.684
2-1	24–42	46	–	35.9	48.6	49.1	0.780	1.062	0.735
2-2	24–42	38	27.1	29.8	–	–	0.749	–	–
3-1	22–46	50	33.2	36.8	54.3	59.1	0.700	1.134	0.617
3-3	20–28	20	15.7	18.1	22.1	24.8	0.845	1.173	0.721
4-1	68–84	54	–	–	61.9	62.2	–	1.149	–
4-2	68–84	62	45.1	55.1	71.3	74.6	0.808	1.177	0.687
5-2	64–86	70	39.3	52.1	93.3	94.9	0.653	1.344	0.486
6-1	116–130	80	39.6	–	–	–	0.495	–	–
6-2	135–150	110	51.0	63.2	152.5	158.7	0.519	1.415	0.367

q_{su1}: skin friction values suggested by the Chinese Technical Code for Building Pile Foundations (JGJ 94-2008); q_{su2}: skin friction values obtained from the cone penetration tests (CPTs); q_{su3}: measured values of skin friction ; R_1: average ratio of q_{su3} to q_{su2}; R_2: ratio of the skin friction of the tension pile to that of the compression pile

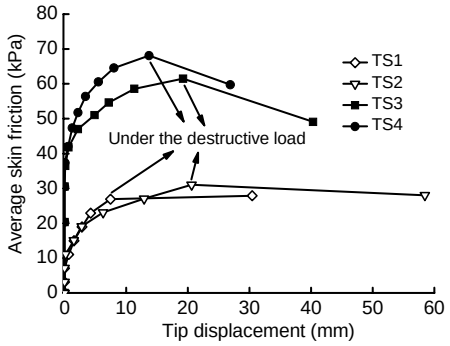

Fig. 6 Average skin friction versus tip displacement under different loads

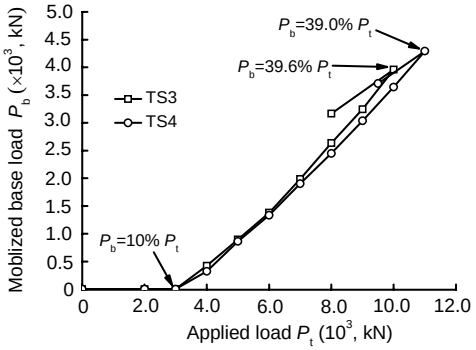

Fig. 7 Mobilized base load versus applied load

4.4 Mobilized base load of piles under compression

The mobilized base load can be approximately estimated from the strain measured by the strain gauge near the tip of each pile. It is easy to understand that the measured tip resistance in two tension piles (TS1 and TS2) is near zero during the whole loading cycle. However, the mobilized base loads of the two piles (TS3 and TS4) under compression increase with increasing applied loads (Fig. 7).

Fig. 7 shows that the base load is gradually mobilized when the applied load is larger than 4000 kN, and more load is transferred to the pile tip with increasing applied loads. The ratio of mobilized base load to applied load increases from 10.0 % to 39.0 %. Unlike the traditional applied load versus base load curve in the non-destructive test (Han and Ye, 2006; Zhang *et al*., 2010), the mobilized base load decreases because of the punching failure at the pile tip under the destructive load, as shown in Fig. 7.

The settlement at the pile tip can be estimated through the solution of a rigid punch acting on an elastic half space, as suggested by Randolph and Wroth (1978):

$$S_b = \frac{P_b(1-\upsilon_b)}{4r_b G_b}, \tag{4}$$

where S_b is the settlement at the pile tip, P_b is the mobilized base load, G_b and υ_b represent the shear modulus and Poisson's ratio of the tip soil (0.3 for gravel in this study), respectively, and r_b is the radius of the pile tip (0.4 m is used in this calculation).

The relationship between base load and tip displacement can be approximately modeled using a secant shear modulus of the tip soil (Han and Ye, 2006):

$$G_b = G_{bi}\left(1 - R_f \frac{P_b}{P_{bmax}}\right)^2, \tag{5}$$

where G_{bi} is the initial shear modulus of the tip soil (1420 and 1540 MPa for TS3 and TS4, respectively), R_f is the failure ratio (0.80 and 0.85 for TS3 and TS4, respectively), and P_{bmax} is the maximum base load (3246 and 4294 kN for TS3 and TS4, respectively).

The theoretical tip displacement-base load curves of the piles TS3 and TS4 are shown in Fig. 8. Before failure of the compression piles is reached, the theoretical tip displacement-base load curves compare well with the measured ones when R_f is 0.80. In the non-destructive test (Zhang *et al*., 2009; 2010), the load-displacement relationship developed at the pile base followed the hardening model. Actually, under the destructive load, the tip displacement-mobilized base load follows a softening model. This finding is useful for revising the evaluation of the bearing capacity of pile and establishing a reasonable load-displacement relationship at the pile tip in numerical analysis.

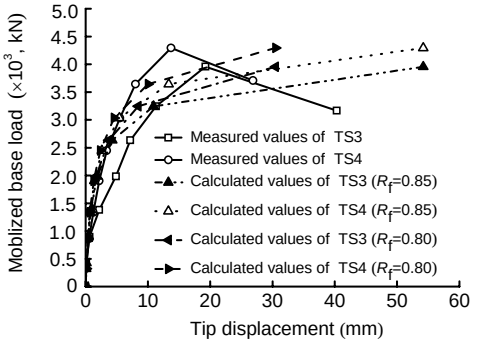

Fig. 8 Tip displacement versus mobilized base load

4.5 Relative displacement between piles and soils

The relative displacement between soil *i* and pile is expressed by

$$\delta_{ui} = S_t - \sum_{j=1}^{i} \frac{L_j}{2}\left(\varepsilon_j + \varepsilon_{j+1}\right), \tag{6}$$

where S_t is the pile head settlement, ε_j is the strain of the reinforcing steel bar (the concrete) located at section *j*, and L_j is the length of the pile length placed in soil layer *j*.

The relationship between the skin friction and pile-soil relative displacement at different depths is shown in Fig. 9.

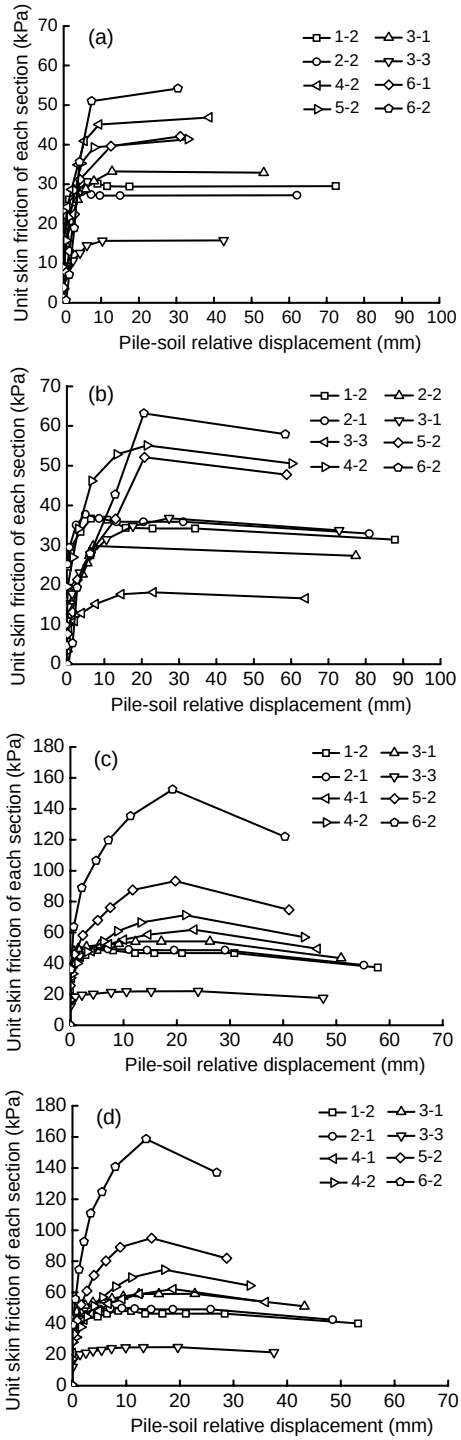

Fig. 9 Unit skin friction versus pile-soil relative displacement: (a) TS1; (b) TS2; (c) TS3; (d) TS4

Fig. 9 shows that the skin friction has a good correlation with the pile-soil relative displacement and decreases from a peak value with increasing loads. The shaft resistance degradation investigated in

the non-destructive tests only existed at a shallow depth, and the skin friction of deeper soil was not fully developed due to less relative displacement between piles and deeper soil (Zhang *et al*., 2009; 2010). Unlike the results of the non-destructive tests, the softening is accompanied by a reduction in skin friction and observed to be along the pile depth. That is, the skin friction along the pile depth approaches to the limited state, and decreases from a peak value with increasing loads.

Fig. 9 also indicates the thresholds of the slip displacement for fully mobilizing the shaft resistances in different soils. The relative displacements between pile and soils corresponding to the limited skin frictions are summarized in Table 5.

Table 5 Thresholds of slip displacement for fully mobilizing skin frictions in different soils

Soil No.	Soil layer	Average relative displacement (mm)	
		TS1 and TS2	TS3 and TS4
1-2	Sandy silt	6.4	6.8
2-1	Sandy silt	4.9	8.1
2-2	Sandy silt	7.0	–
3-1	Silty sand mixed silt	20.1	24.5
3-3	Silt clay	16.7	21.8
4-1	Silty clay	–	21.0
4-2	Silty clay	15.4	19.4
5-2	Fine sand	14.4	17.2
6-1	Gravel	12.6	–
6-2	Gravel	14.0	16.5

The thresholds of the slip displacement for fully mobilizing the shaft resistances in the uplift cases are smaller than those in the piles under compression. Generally, the thresholds of the relative pile-soil displacement for fully mobilizing skin frictions of the tension piles in the sandy silt, silty sand mixed silt, silt clay, silty clay, fine sand, and gravel are about 6, 20, 16, 15, 14, and 13 mm, respectively, whereas the skin frictions of the pile under compression are close to the limit values when the pile-soil relative displacements in the sandy silt, silty sand mixed silt, silt clay, silty clay, fine sand, and gravel are about 7, 24, 22, 19, 17, and 16 mm, respectively. This is an explanation for the lower limited skin friction in the piles under tension, which is useful for estimating the ultimate shaft resistance in numerical analysis.

5 Conclusions

In this paper, four destructive full-scale pile loading tests were conducted to investigate the field performance of the long bored piles under tension and compression. The observations have provided some key findings summarized below.

1. The measured skin frictions for the piles under compression are about 6% to 42% higher than the values estimated from CPTs, whereas the measured values of the uplift cases are about 16% to 50% smaller than the estimated values from CPTs. Moreover, the average limiting skin frictions of the tension piles are about 0.36 to 0.78 times the average ultimate skin frictions of the piles under compression.

2. The ratio of mobilized base load to applied load increases from 10.0% to 39.0 %. Unlike the applied load-mobilized base load curve in the non-destructive test, the mobilized base load decreases because of the punching failure at the pile tip under the destructive load.

3. Before failure of the compression pile is reached, the theoretical tip displacement-mobilized base load curves compare well with the measured ones when R_f is 0.80. Actually, in the destructive test, the tip displacement-base load follows a softening model. This finding is useful for revising the evaluation of the bearing capacity of pile and establishing a reasonable load-displacement relationship at the pile tip in numerical analysis.

4. The ultimate pile-soil relative displacements for completely mobilizing the shaft resistance in the uplift cases are found to be smaller than those in the piles under compression, and the thresholds of slip displacement for fully mobilizing the skin frictions in different soils are summarized in this paper. These findings are useful in the analysis of the pile load-settlement response.

References

Ai, Z.Y., Han, J., 2009. Boundary element analysis of axially loaded piles embedded in a multi-layered soil. *Computer and Geotechnics*, **36**(3):427-434. [doi:10.1016/j.compgeo.2008.06.001]

Das, B.M., 1983. A procedure for estimation of uplift capacity of rough piles. *Soils and Foundations*, **23**(3):122-126.

Guo, W.D., Randolph, M.F., 1999. An efficient approach for settlement prediction of pile groups. *Geotechnique*, **49**(2): 161-179. [doi:10.1680/geot.1999.49.2.161]

Han, J., Ye, S.L, 2006. A field study on the behavior of micropiles in clay under compression or tension. *Canadian Geotechnical Engineering*, **43**(1):19-29. [doi:10.1139/T05-089]

JGJ 106-2003. Technical Code for Testing of Building Foundation Piles. China Construction Industry Press, Beijing, China, p.22-26 (in Chinese).

JGJ 94-2008. Technical Code for Building Pile Foundation. China Architecture and Building Press, Beijing, China, p.33-34 (in Chinese).

Kraft, L.M., Ray, R.P., Kakaaki, T., 1981. Theoretical *t-z* curves. *Journal of Geotechnical Engineering Division*, **107**(11):1543-1561.

Lai, Y., Jin, G.F., 2010. Uplift behavior and load transfer mechanism of prestressed high-strength concrete piles. *Journal of Central South University of Technology*, **17**(1):136-141. [doi:10.1007/s11771-010-0022-6]

Prakash, S., Sharma, H.D., 1990. Pile Foundation in Engineering Practice. John Wiley & Sons, New York, USA, p.824.

Randolph, M.F., Wroth, C.P., 1978. Analysis of deformation of vertically loaded pile. *Journal of the Geotechnical Engineering Division*, **104**(12):1465-1488.

Randolph, M.F., Worth, C.P., 1979. An analysis of the vertical deformation of pile groups. *Geotechnique*, **29**(4):423-439. [doi:10.1680/geot.1979.29.4.423]

Said, I., De, G.V., Frank, R., 2009. Axisymmetric finite element analysis of pile loading tests. *Computer and Geotechnics*, **36**(1-2):6-19. [doi:10.1016/j.compgeo.2008.02.011]

Shanker, K., Basudhar, P.K., Patra, N.R., 2007. Uplift capacity of single piles: predictions and performance. *Geotechnical and Geological Engineering*, **25**(2):151-161. [doi:10.1007/s10706-006-9000-z]

Xiao, H.B., Luo, Q.Z., Tang, J., Li, Q.S., 2002. Prediction of load-settlement relationship for large-diameter piles. *Structure Design of Tall Buildings*, **11**(4):285-293. [doi:10.1002/tal.201]

Zhang, Z.M., Zhang, Q.Q., Zhang G.X., 2009. Mechanical properties of uplift pile in soft soils. *Journal of Zhejiang University (Engineering Science)*, **43**(11):2114-2119 (in Chinese).

Zhang, Z.M., He, J.Y., Zhang, Q.Q., Zeng L.C., 2010. Measured settlements of super-long piles and pile groups for a building of 323 m in height in Wenzhou. *Chinese Journal of Geotechnical Engineering*, **32**(3):330-337 (in Chinese).

Zhu, H., Chang, M.F., 2002. Load transfer curves along bored piles considering modulus degradation. *Journal of Geotechnical and Geoenvironmental Engineering*, **128**(9):764-774. [doi:10.1061/(ASCE)1090-0241(2002)128:9(764)]